Anesthesiology 2010; 113:134–46

Calcium Signaling in Intact Dorsal Root Ganglia

New Observations and the Effect of Injury

Geza Gemes, M.D.,* Marcel Rigaud, M.D.,* Andrew S. Koopmeiners, B.S.,† Mark J. Poroli, B.S.,‡ Vasiliki Zoga, M.D.,§ Quinn H. Hogan, M.D.‖

ABSTRACT

Background: Ca^{2+} is the dominant second messenger in primary sensory neurons. In addition, disrupted Ca^{2+} signaling is a prominent feature in pain models involving peripheral nerve injury. Standard cytoplasmic Ca^{2+} recording techniques use high K^+ or field stimulation and dissociated neurons. To compare findings in intact dorsal root ganglia, we used a method of simultaneous electrophysiologic and microfluorimetric recording.

Methods: Dissociated neurons were loaded by bath-applied Fura-2-AM and subjected to field stimulation. Alternatively, we adapted a technique in which neuronal somata of intact ganglia were loaded with Fura-2 through an intracellular microelectrode that provided simultaneous membrane potential recording during activation by action potentials (APs) conducted from attached dorsal roots.

Results: Field stimulation at levels necessary to activate neurons generated bath pH changes through electrolysis and failed to predictably drive neurons with AP trains. In the intact ganglion technique, single APs produced measurable Ca^{2+} transients that were fourfold larger in presumed nociceptive C-type neurons than in nonnociceptive Aβ-type neurons. Unitary Ca^{2+} transients summated during AP trains, forming transients with amplitudes that were highly dependent on stimulation frequency. Each neuron was tuned to a preferred frequency at which transient amplitude was maximal. Transients predominantly exhibited monoexponential recovery and had sustained plateaus during recovery only with trains of more than 100 APs. Nerve injury decreased Ca^{2+} transients in C-type neurons, but increased transients in Aβ-type neurons.

Conclusions: Refined observation of Ca^{2+} signaling is possible through natural activation by conducted APs in undissociated sensory neurons and reveals features distinct to neuronal types and injury state.

What We Already Know about This Topic

- Intracellular calcium concentration is an important second messenger in sensory neurons
- Traditional stimulation of sensory neurons in acute cultures by electrical fields has several drawbacks

What This Article Tells Us That Is New

- Recordings from neurons in intact ganglia reveal that each neuron type has a distinct firing frequency at which the calcium signal is maximized and that calcium is elevated even by single action potentials, particularly in slow conducting nocicepetive neurons

UNDERSTANDING the function of the peripheral sensory neuron is central to the science of anesthesia. Not only does activation of sensory neurons initiate the neurophysiologic events that trigger pain, but also other sensory neurons modulate reflexes that control muscle tone, ventilation, and thermoregulation during and after anesthesia. Also, temporary interruption of sensory neuron function is the core requirement of regional anesthesia. Furthermore, dysfunction of sensory neurons is a cause of neuropathic pain

◆ This article is accompanied by an Editorial View. Please see: Gold MS: Beyond the lamppost: Approaches to answering the questions of interest. ANESTHESIOLOGY 2010; 113:7–9.

* Research Fellow, Department of Anesthesiology, Medical College of Wisconsin, Milwaukee, Wisconsin, and Resident, Department of Anesthesiology, Medical University of Graz, Graz, Austria. † Medical Student, ‡ Research Technician, § Research Fellow, Department of Anesthesiology, Medical College of Wisconsin. ‖ Professor, Department of Anesthesiology, Medical College of Wisconsin, and Anesthesiologist, Zablocki Veterans Affairs Medical Center, Milwaukee, Wisconsin.

Received from the Department of Anesthesiology, Medical College of Wisconsin, Milwaukee, Wisconsin. Submitted for publication August 29, 2009. Accepted for publication February 15, 2010. Supported by grant NS-42150 from the National Institute of Neurological Disorders and Stroke, National Institutes of Health, Bethesda, Maryland (to Dr. Hogan), and an Erwin Schroedinger Fellowship (project J2695) from the Austrian Science Fund, Vienna, Austria (to Dr. Rigaud). Presented in part at the American Society of Anesthesiologists Annual Meeting, San Francisco, California, October 13–17, 2007.

Address correspondence to Dr. Hogan: Anesthesiology Research, MEB M4280 Medical College of Wisconsin, 8701 Watertown Plank Road, Milwaukee, Wisconsin 53226. qhogan@mcw.edu.

syndromes that are especially challenging to treat. These neurons serve their primary task of providing the central nervous system with environmental and internal information by selectively generating and transmitting action potentials (APs) in response to mechanical, thermal, and chemical stimuli. In addition to this electrophysiologic function of the neuronal membrane, important cytoplasmic and nuclear functions are regulated by the critical chemical messenger Ca^{2+}, an ion that regulates such diverse events as neuronal differentiation, gene expression, neurotransmitter release, excitability, and apoptosis.[1] The increase and decrease in the cytoplasmic Ca^{2+} transient that follows membrane depolarization are initiated by influx through the membrane and are further shaped by release from intracellular stores, sequestration into organelles, and extrusion from the cell. Better understanding of these complex events in sensory neurons is essential to devising safer local anesthetics and more effective chronic pain treatments.[2,3]

Standard techniques have been used to explore cytoplasmic Ca^{2+} signaling in sensory neurons using Ca^{2+}-sensitive fluorophores and advanced cameras. Most often, sensory neuron somata are dissociated from the dorsal root ganglion (DRG) and thereafter activated by membrane depolarization using increased bath K^+ concentration or field stimulation. Although this model has yielded useful insights, there are significant limitations. The timing of activation by K^+ is limited to applications of at least a few seconds. This duration of exposure results in sustained membrane depolarization that may model events at transduction sites in the periphery, but is massively prolonged compared with trains of AP depolarizations that each last only a few milliseconds. Field stimulation, by which electrical current is passed between electrodes in a bath containing the neurons, has been devised to address this limitation.[4] However, there are theoretical concerns. Application of voltage greater than 1.23 V, the standard potential of water at 25°C, drives decompensation of water by the process of electrolysis that generates hydrogen at the anode. Further, in saline solutions, oxidation of chloride ions to chlorine gas may occur at the anode. Although dissociation and culturing of DRG neurons are also a part of the standard technique, removal of the axon from the sensory neuron soma eliminates as much as 99.8% of the volume of the cell.[5] In addition, the neurons are deprived of their natural environment by removal of the surrounding envelope of closely apposed satellite glial cells,[6] and digestion may affect membrane proteins, which in turn alters neuronal function.[7]

Accordingly, in addition to examining neuronal performance under customary dissociation, bath, and stimulation conditions, the experiments described here were designed to adapt elements of various techniques to develop and test a method for recording Ca^{2+} signals in sensory neurons with improved physiologic relevance while avoiding the limitations noted above. Our overall purpose was to provide improved tools for exploring sensory neuron function in anesthesia-related topics. Because nerve injury produces substantial derangement of sensory neurons Ca^{2+} signals,[8–11] we examined this condition as an exercise in applying our improved technique.

Materials and Methods

Animal Subjects

All procedures were approved by the Animal Care Committee of the Medical College of Wisconsin, Milwaukee, Wisconsin. Male Sprague–Dawley rats (150 g; Taconic Farms, Inc., Hudson, NY) received anesthesia (2% isoflurane in oxygen), skin incision, and skin stapling in the control group, whereas the spinal nerve ligation neuropathic pain model was used in others for which the sixth lumbar (L6) transverse process was removed, and the L5 and L6 spinal nerves were ligated with 6–0 silk ligature and transected.[12] Sensory function was evaluated by determining the behavioral response to noxious punctate mechanical stimulation that was produced by applying a 22-gauge spinal anesthesia needle to the plantar surface of the hindpaw with pressure adequate to indent but not penetrate the skin.[13] The frequency of either a brief withdrawal or a sustained paw lifting, shaking, and grooming (hyperalgesia-type behavior) was determined during 10 touches on each of the three occasions between 10 and 17 days after surgery. For spinal nerve ligation rats, only those with more than 20% hyperalgesic response rate were studied in the experiments described below.

Preparation of Tissues

For dissociation, ganglia were harvested rapidly after decapitation. The fourth and fifth lumbar DRGs were incubated in 0.01% blendzyme-2 (containing collagenase and neutral protease; Roche Diagnostics, Indianapolis, IN) for 30 min followed by incubation in 0.25% trypsin (Sigma Aldrich, St. Louis, MO) and 0.125% DNase (Sigma) for 30 min, both dissolved in Dulbecco's modified Eagle's medium/F12 with glutaMAX (Invitrogen, Carlsbad, CA). After exposure to 0.03% trypsin inhibitor and centrifugation, the pellet was gently triturated in culture medium containing Neural Basal Media A with B27 supplement (Invitrogen), 0.5 mM glutamine, 10 ng/ml nerve growth factor 7S (Alomone Labs, Jerusalem, Israel), and 0.02 mg/ml gentamicin (Invitrogen). Neurons were plated onto poly-L-lysine-coated glass cover slips (Deutsches Spiegelglas; Carolina Biologic Supply, Burlington, NC), maintained at 37°C in humidified 95% air and 5% CO_2 for 2 h, and were studied no later than 6 h after harvest. Alternatively, intact ganglia with dorsal roots attached were harvested by laminectomy during isoflurane anesthesia and placed in artificial cerebrospinal fluid (128 mM NaCl, 3.5 mM KCl, 1.2 mM $MgCl_2$, 2.3 mM $CaCl_2$, 1.2 mM NaH_2PO_4, 24.0 mMC $NaHCO_3$, 11.0 mM glucose) bubbled by 5% CO_2 and 95% O_2 to maintain a pH of 7.35.

Electrophysiologic Recording

Intracellular recordings were performed with microelectrodes fashioned from borosilicate glass with an Omega dot

fiber (FHC, Bowdoin, ME) with resistances of 80–120 mΩ when filled with 2 M potassium acetate buffered to pH 7.6, mounted in a holder with a sideport to release luminal pressure. Dissociated neurons were superfused with Tyrode's solution (140 mM NaCl, 4 mM KCl, 2 mM $CaCl_2$, 10 mM glucose, 2 mM $MgCl_2$, 10 mM HEPES) at room temperature, whereas intact ganglia were superfused with artificial cerebrospinal fluid regulated to 35°C with an inline heat exchanger, and both solutions were delivered at 3 ml/min. (Noncomparable solutions were used for dissociated neurons and intact tissue to optimize preparation stability and to replicate customary use.) Lidocaine was administered through a microperfusion pipette stationed 100 μm from the tissue, with flow driven by pressure from a valve system (IIe, Toohey Company, Fairfield, NJ). The DRG was stabilized in the chamber with an anchor fashioned from gold wire holding parallel strands of 10–0 polypropylene monofilament at 1-mm intervals. Superficial neurons in the first or second layer were impaled while observed with an upright microscope (Eclipse E600FN; Nikon USA, Melville, NY) equipped with differential interference contrast optics and infrared illumination through a 40× water immersion objective (Nikon Fluor 40×/0.8W). Membrane potential was recorded using an active bridge amplifier (Axoclamp 2B; Axon Instruments, Molecular Devices, Sunnyvale, CA), filtered at 10 kHz, and digitized at 40 kHz (Digidata 1322A, Axon Instruments and Axograph × 1.1; Axograph Scientific, Sydney, Australia). Recording was initiated after resting membrane potential had stabilized (3 min) to less than −50 mV. Data were obtained only from neurons in which membrane potential remained stable, in which APs could clearly be discerned from the stimulus artifact, and in which an AP amplitude was greater than 45 mV. Leakage of neuronal contents after withdrawal of the electrode conceivably could alter function of adjacent neurons for which reason only nonadjacent neurons were examined.

Neuronal Activation

Dissociated neurons were activated by one of the two techniques. Field stimulation was achieved using either a constant voltage stimulator built in-house that delivered 1-ms pulses at 0–30 V, monitored continuously, or a constant current stimulator (SIU-102, Warner Instruments, Hamden, CT). Coverslips carrying neurons were mounted in a 260-μl chamber (Warner RC-21BFRS), and stimuli were delivered either through the two built-in platinum electrodes (10 mm long, 6-mm separation) or through a custom-made pair of silver electrodes (5 mm long, 3-mm separation). Alternatively, impaled neurons were stimulated by delivery of depolarizing current through the stimulating electrode. Neurons in intact ganglia were activated by APs conducted from a stimulation site on the proximal end of attached dorsal roots in which a pair of platinum wire electrodes connected to an isolated current source (in-house design) delivered 0.06–1 ms pulses at 1.5× threshold for just generating an AP. Conduction velocity (CV) was measured by dividing the distance between stimulation and recording sites by the conduction latency.

Microfluorometric $[Ca^{2+}]_c$ Determination

The Ca^{2+}-sensitive fluorophore Fura-2 was loaded into neurons by one of the two techniques. Dissociated neurons were incubated for 30 min in Fura-2-AM (5 μM; Invitrogen) in Tyrode's solution, followed by Tyrode's alone for 30 min. A technique previously reported for loading a fluorophore into other neuronal tissues[14,15] was adapted for neurons in intact ganglia. Neurons were loaded directly from the recording microelectrode filled with 10 mM Fura-2, a concentration recommended by the manufacturer (Invitrogen) and used by others for loading by microelectrode impalement,[14,15] dissolved in 2 M potassium acetate (pH 7.6 with HEPES).

Cells were imaged through a 20× or 40× objective, using a cooled 12-bit charge-coupled device camera (Coolsnap fx; Photometrics, Tucson, AZ). Excitation was achieved at 340 and 380 nm with a 150 W xenon lamp (Lambda DG-4; Sutter, Novato, CA), and images were collected at 510 nm using Metaflour software (Molecular Devices, Downingtown, PA). The ratio of fluorescent intensity at these wavelengths ($R = I_{340}/I_{380}$) was determined on a pixel-by-pixel basis for individual neurons after background subtraction. $[Ca^{2+}]_c$ was estimated by the formula $[Ca^{2+}]_c = K_d \cdot \beta \cdot (R - R_{min})/(R_{max} - R)$, where $\beta = (I_{380\ max})/(I_{380\ min})$, $K_d = 224$ nM.[16] R_{min}, R_{max}, and β were determined separately for dissociated neurons (0.38, 8.49, and 9.54, respectively; n = 33) and for intact ganglion recording (0.313, 11.28, and 28.64, respectively; n = 3). Ionomycin (5 μM for dissociated, 80 μM for intact DRG; Calbiochem, Gibbstown, NJ) in Ca^{2+}-free bath produced a stable R_{min}, indicating equilibrium with bath solution, and exposure to Tyrode's solution with ionomycin produced R_{max}.[8] Although we report $[Ca^{2+}]_c$ rather than fluorescence ratios, it should be noted that Ca^{2+} concentrations more than 1 μM determined by Fura-2 become less reliable. No single fluorophore is fully reliable across the entire range of possible cytoplasmic Ca^{2+} concentrations, but Fura-2 was chosen because of its optimal performance at $[Ca^{2+}]_c$ near the neurons' resting level. Dimensions of cytoplasmic Ca^{2+} signals are reported as amplitude of the activity-induced transient. Recovery of the transient in the form of decay time constant was determined for transients that resolved in a simple monoexponential fashion.

Statistical Analysis

Dissociated neurons were chosen in the 30- to 35-μm diameter size range, whereas CV was used to categorize neurons in intact ganglia[17] because this tends to segregate neurons with specific receptive field properties.[18,19] Specifically, neurons with dorsal root CV less than 1.5 m/s were considered C-type, those with CV more than 15 m/s were considered Aβ-type, and neurons with CV more than 1.5 m/s but CV less than 10 m/s were considered Aδ-type. For neurons with CV between 10 and 15 m/s, long AP duration was used to classify the cells as Aδ-types.[17] Data are expressed as mean ± SEM.

Student *t* test (paired and unpaired), one-way ANOVA, and two-way ANOVA, with repeated measures if appropriate, were used (Statistica; StatSoft, Inc., Tulsa, OK) to detect differences in measured parameters between injury groups and stimulation protocols. *Post hoc* testing was performed with paired comparisons by least-square differences with Bonferroni's correction for multiple comparisons. In many cases, data for more than one protocol were obtained from a single neuron. To describe the stability of transient dimensions with repetition, we subtracted each measurement from the average of the repeated measurements and averaged the absolute value of this difference. To describe variability of the decay time constant of a neuron (τ) across different stimulation frequencies (7, 20, 50, and 100 Hz), the τ of a neuron at frequency f (τ^f) was normalized to the average across frequencies of that neuron ($\tau^f_{nl} = \tau^f/([\tau^7 + \tau^{20} + \tau^{50} + \tau^{100}]/4)$), then these were averaged for all neurons at a given frequency (τ^f_{AVG}), which established the overall trend due to the effect of frequency. To describe the variation of a given neuron while accounting for the overall effect of frequency, we calculated the squared difference between the time constant and τ^f_{AVG} of a neuron at each frequency, which was then summed across the four tested frequencies and divided by the degrees of freedom (*i.e.*, $\Sigma^{f=7,20,50,100\ Hz}(\tau^f_{nl} - \tau^f_{AVG})^2]/3$), which is called as normalized variance hereafter. Significance was accepted at $P < 0.05$.

Results

A total of 40 rats were used, 11 of which had spinal nerve ligation surgery, whereas 29 had skin incision only. Rats with spinal nerve ligation had a frequency of hyperalgesia-type responses to noxious mechanical stimulation of 39.8 ± 15.3%, whereas control animals had 0.0 ± 0.0 ($P < 0.001$).

Field Stimulation of Dissociated Neuronal Somata

Resistance between the field stimulation electrodes built into the chamber was 0.9–1.1 MΩ, and the resistance for the custom electrodes was 5.1 MΩ. Ca^{2+} responses were maximal at voltages (recorded online) of 25–30 V. Close examination of the stimulating wires demonstrated accumulation of bubbles visible under 100× magnification even after two trains of 21 stimuli of 1-ms duration (fig. 1A). Indicator paper placed in the recording chamber to measure pH showed reciprocal color changes at the electrodes after the same stimulation, indicating pH values of less than 4 and more than 11 in the region of the electrodes (fig. 1B). We recorded the potential in the bath during field stimulation using either a low-resistance glass electrode (500 kΩ) attached to the electrophysiologic amplifier or a wire electrode connected to a digital oscilloscope. Both pulse generators and both stimulating electrode systems produced sustained bath potentials that fused into a continuous field potential with pulse durations of either 0.1 or 1 ms at 7 Hz (fig. 1C). Findings (data not shown) were similar with a biphasic stimulus pulse.

To identify the limits of field stimulation to generate trains of neuronal activity in neurons dissociated from adult rats, we tested the effect of stimulation frequency on Ca^{2+} transient dimensions in dissociated control neurons (21 stimuli; 1-ms duration; 7, 20, 50, and 100 Hz in a random order; fig. 1D). Under these conditions, 11% (7/65) of neurons failed to respond at all, indicating highly variable response to field stimulation. In the remaining neurons, transient amplitude declined as stimulation frequency increased ($P < 0.01$, 40% decrease between 20 and 100 Hz; fig. 1E). If transient amplitude represents the summation of individual excitatory events, this finding could in part be due to a failure of field stimulation to activate neurons at higher stimulation frequencies. Although stimulation frequency had no effect on the average decay time constant, the decay time constant of individual neurons at different frequencies showed a large variability (fig. 1E). Specifically, the normalized variance of decay time constant of each neuron across the four frequencies was 13 ± 3%.

Intracellular Stimulation of Dissociated Neuronal Somata

A possible explanation for the decline in $[Ca^{2+}]_c$ transients with higher frequencies is that neuronal somata are not able to sustain firing rates beyond 20 Hz. To test this, we used direct intracellular current injection through a recording electrode to excite neurons that had been loaded by bath Fura-2-AM.[20] Somatic APs were discerned in all neurons (n = 7), and each of the 21 stimuli produced an AP in trains at 7, 20, 50, and 100 Hz (fig. 2A). In contrast to field stimulation, simultaneous $[Ca^{2+}]_c$ recording during direct stimulation showed no decrease in transient amplitude ($P = 0.35$, 7% difference between averages at 20 and 100 Hz, fig. 2B). The decay time constant was also not affected by frequency and had a normalized variance for each neuron across the four frequencies of 8 ± 3%. These findings indicate that adult rat sensory neuron somata are intrinsically able to generate APs at rates up to 100 Hz. If field stimulation were able to trigger APs at these same stimulation frequencies, comparable transient amplitudes should be generated. The significantly smaller transients ($P < 0.01$) and the 40% fall-off of transient amplitude with increasing frequency are strong evidences of a progressive failure of field stimulation to generate APs at frequencies at which the neurons are capable of firing.

Intracellular Stimulation of Neuronal Somata in Intact Ganglia

Because dissociation alters the neuronal environment, traumatizes the neuron, and may digest cellular surface proteins, findings such as ability to fire at high frequencies could be dissociation-induced artifacts. Therefore, we developed a technique for imaging $[Ca^{2+}]_c$ in intact DRGs (fig. 2C). Dye loading with bath-applied Fura-2-AM proved unfeasible because individual neuronal profiles could not be identified during the fluorimetric recording (data not shown). Also,

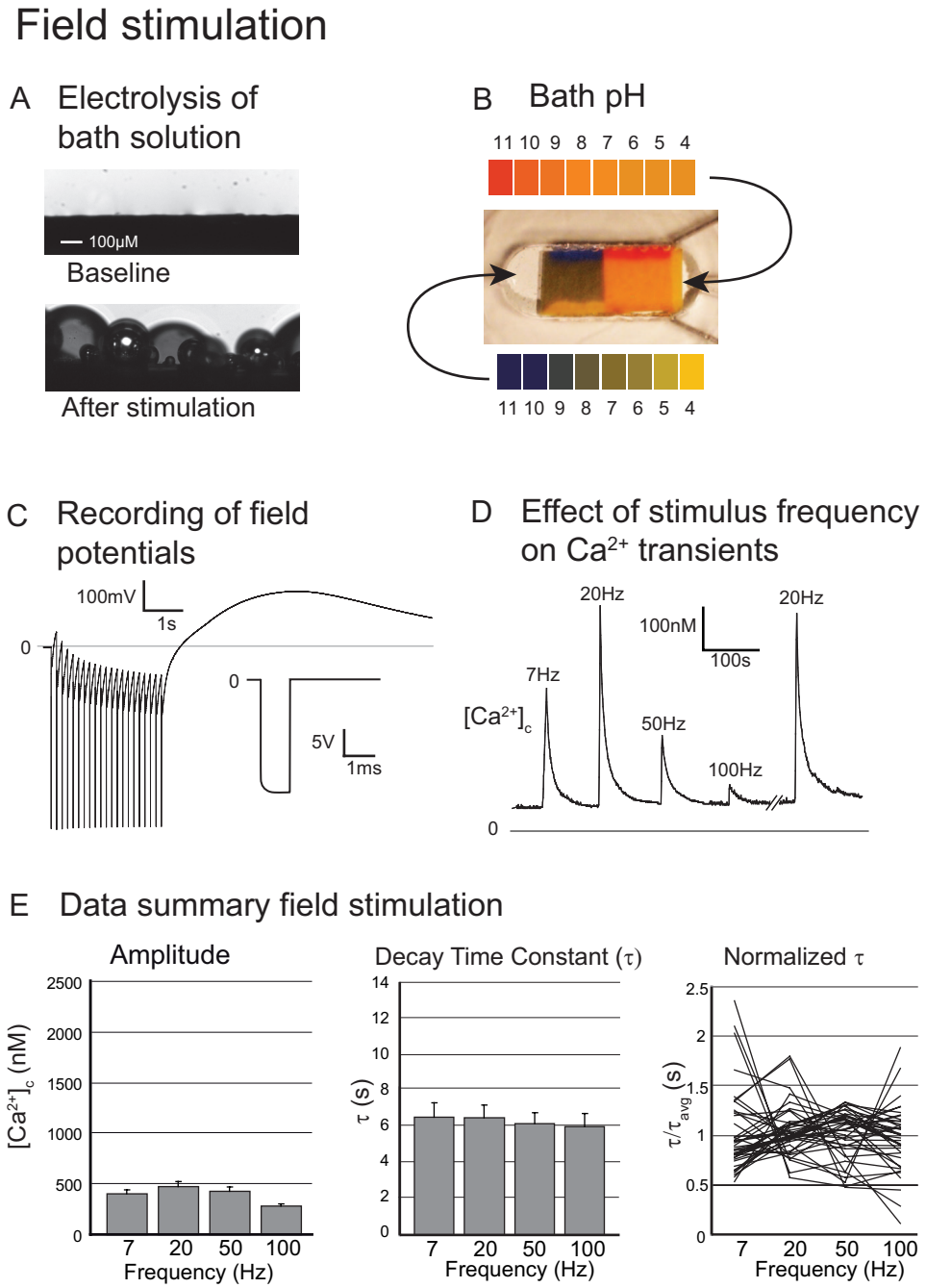

Fig. 1. Field stimulation. (*A*) Electrolysis of bath solution by field stimulation (2 trains of 21 pulses, 1 ms each) generates gas bubbles at both electrodes. The edge of the electrode seems as a dark band at baseline conditions, but is obscured by bubbles after stimulation. (*B*) Field stimulation (8 trains of 21 pulses, 1 ms each) produces pH of more than 11 and less than 4 on pH indicator paper inserted into the tissue bath. The two electrodes can be seen entering the top right and bottom right of the image and aligning with the edges of the pH-sensitive paper, which has right and left sections with different color ranges. The color code on the top corresponds to the right section of the pH indicator paper strip, and *vice versa*. (*C*) Recording of the voltage in the bath during a stimulus train (21 pulses at 7 Hz, 1-ms pulses, SIU-102 stimulator, RC-21BRFS recording chamber; Warner Instruments, Hamden, CT) with a low-resistance (500 kΩ) recording electrode. *Inset*: recording of voltage at the stimulating electrodes. The field voltage accumulates during stimulator pulses and remains elevated several seconds after the last stimulus. (*D*) Typical recording of cytosolic Ca^{2+} transients from a control neuron using activation by field stimulation (21 pulses, 2 ms each) at four different frequencies. (*E*) Summary data of recordings of that shown in *D*. Transient amplitude (*left*) reaches a peak at stimulation frequencies greater than 20 Hz and then declines ($P < 0.001$, repeated-measures analysis of variance main effect, n = 58). Although the average decay time constant does not change with frequency (*middle*, n = 42), the individual line plots of decay constants (normalized to the average across frequencies, *right*) show substantial variability and inconsistency across stimulation frequencies.

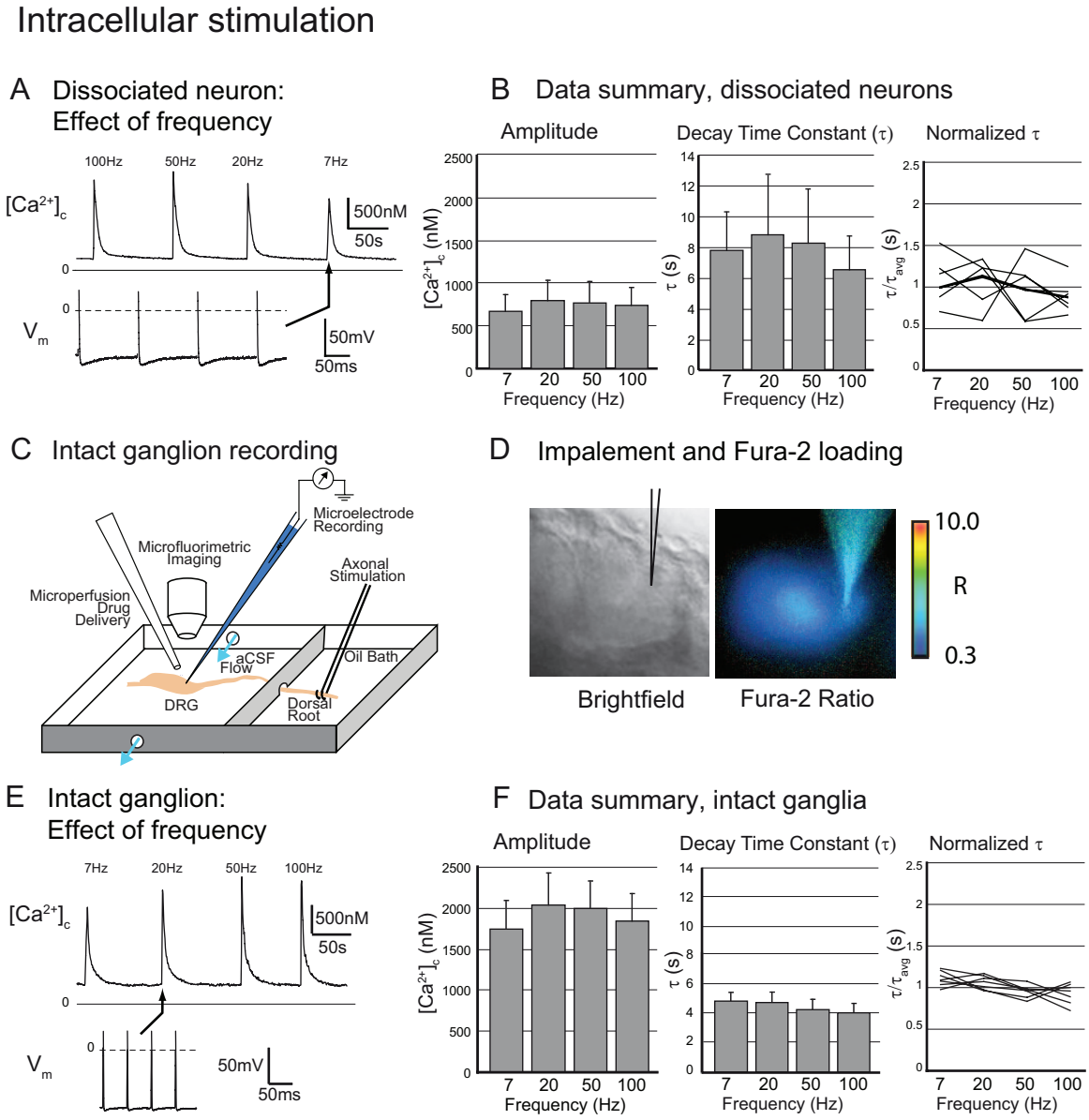

Fig. 2. Intracellular stimulation. (*A*) Typical recording of cytosolic Ca^{2+} transients (*upper trace*) from a dissociated control neuron at room temperature, activated by current injection through the intracellular recording electrode with pulse trains (21 stimuli, 1 ms each) at four different frequencies. Simultaneous recording from the electrode (*lower trace*) confirms the generation of an action potential after each stimulus. (*B*) Summary data from recordings such as that shown in *A*, from seven control neurons. Ca^{2+} transient amplitude and decay constant do not change with stimulation frequency (analysis of variance main effect $P = 0.35$ and $P = 0.96$). Line plots of normalized decay constants (*right*) demonstrate moderate variability across stimulation frequencies. (*C*) Schematic drawing of the experimental setup for intact ganglion recording. (*D*, *left*) Brightfield image of a neuron in an intact ganglion (*left*) impaled by the recording pipette (*black outline*). Fluorometric image (*right*) of the same neuron after loading with Fura-2 through the recording electrode. The portion of the recording electrode that is out of the plane of focus is widened by distortion. The *color bar* indicates fluorescence ratios (see text). (*E*) Typical recording of cytosolic Ca^{2+} transients from a neuron in an intact ganglion activated by current injection through the intracellular recording electrode with pulse trains (21 stimuli, 1 ms each) at four different frequencies. Simultaneous recording from the electrode (*lower trace*, showing a portion of a pulse train) confirms the generation of an action potential after each stimulus. (*F*) Summary data of recordings such as that shown in *E*, from seven control neurons. Amplitude reaches a maximum at 20 Hz and then declines (analysis of variance main effect, $P = 0.018$), whereas decay constants decline with increasing frequency ($P = 0.012$). Line plots of normalized decay constants display minimal variability across stimulation frequencies (compare with figs. 1E and 2B). aCSF = artificial cerebrospinal fluid; DRG = dorsal root ganglion.

Fura-2-AM has been shown to preferentially enter satellite glial cells that surround the neuronal somata.[21] To overcome this, we loaded individual somata with Fura-2 *via* the impaling microelectrode, which restricted the fluorescent responses to the single recorded neuron (fig. 2D) and has the added benefit of avoiding accumulation of fluorophore in intracellular organelles as may occur with bath-applied Fura-2-AM loading. The fluorophore entered the cell through passive diffusion alone in 76% of neurons and developed maximum fluorescence intensity within the 3 min required to achieve stable electrophysiologic recordings. In 19% of the neurons, fluorophore loading required a further 529 ± 443 s to reach peak fluorescence, during which fluorescence intensity (380 nm) increased by 58 ± 66%. In 5% of neurons, adequate Fura-2 loading required brief pulses of hyperpolarizing or oscillating current to the recording electrode, despite good electrical recording. Iontophoresis has been used by others for dye loading,[15] whereas the efficacy of electrical oscillation that we observed is unexplained. Loading by these techniques produced fluorescence levels comparable with bath loading, indicating comparable final cytoplasmic Fura-2 levels in the two loading methods. As in dissociated neurons, intracellular stimulation produced somatic APs that were clearly recorded in each of the seven control neurons (fig. 2E). Ca^{2+} transient amplitude was highest at 20 Hz and then declined slightly with higher stimulation frequencies ($P < 0.05$, 7% difference between averages at 20 and 100 Hz), as did the decay time constant (fig. 2F). Generally, Ca^{2+} transients in intact ganglia had higher amplitudes than in dissociated neurons ($P = 0.006$), comparable decay time constants ($P = 0.24$), and lower variability (normalized variance of decay time constant of each neuron across the four frequencies was 1 ± 0%, $P < 0.05$). These effects may be due to the influence of dissociation or alternatively to the differences in bath conditions (temperature and composition).

Axonal Stimulation of Neuronal Somata in Intact Ganglia

To examine cytoplasmic Ca^{2+} signaling under the more physiologic conditions, we altered the above-described technique by inducing somatic APs through conducted axonal APs initiated by dorsal root stimulation, which was used in preference to spinal nerve stimulation so that neurons from the spinal nerve ligation model could be studied. Although the APs conveyed to the soma by this technique travel retrograde compared with normal sensory conduction, the only reported difference from peripheral nerve stimulation is a somewhat slower CV.[22] Simultaneous recordings of fluorometric and electrophysiologic events triggered by conducted APs were obtained from 117 neurons. All neurons that generated APs produced fluorometric Ca^{2+} transients.

To confirm that transients generated using this simultaneous recording technique possess features expected of AP-induced neuronal activation, we demonstrated that transients were nearly eliminated in Ca^{2+}-free bath solution while APs were still present in the simultaneous electrophysiologic traces (fig. 3A), indicating that Ca^{2+} entry through

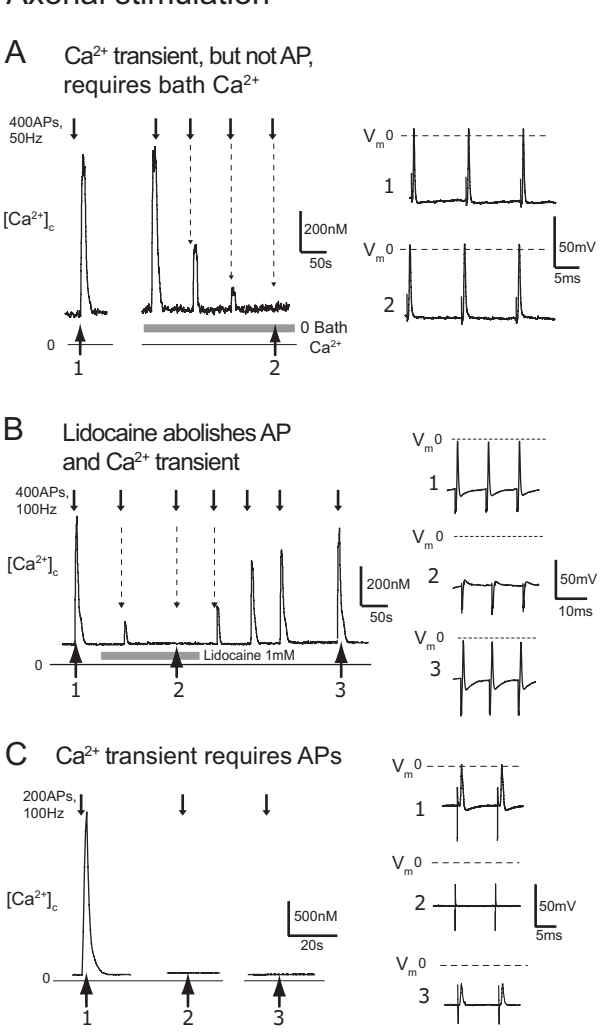

Fig. 3. Simultaneous fluorometric and electrophysiologic recording in neurons of intact ganglia. Cytosolic Ca^{2+} transients in the neuronal soma (*left*) are generated by action potentials (APs) triggered by dorsal root stimulation (*downward arrows*). Simultaneous recording of the membrane potential (*right*, correlating with numbered *upward arrows* in *left*) identifies the presence or absence of AP invasion into the soma. (*A*) Withdrawal of bath Ca^{2+} abolishes the Ca^{2+} transient despite persistence of APs (trace 2). (*B*) Bath-applied lidocaine (1 mM) blocks the transmission of APs (trace 2), which abolish the Ca^{2+} transient; typical of n = 6. (*C*) Only APs elicit a Ca^{2+} transient (trace 1). Subthreshold stimulation that does not produce APs is not accompanied by an increase in cytosolic Ca^{2+} (trace 2). An electrotonic residue from an AP that fails to invade the soma also does not produce a somatic Ca^{2+} transient (trace 3).

voltage-gated Ca^{2+} channels is necessary for initiation of the transient. Elimination of APs with lidocaine also abolishes the Ca^{2+} transient and thus further demonstrates the dependence of Ca^{2+} transients on APs in this model (fig. 3B). Also, failure of AP conduction into the soma, revealed as a reduced electrotonic residue passively conducted from the distant failure site,[23] was associated with failure to produce a Ca^{2+} transient (fig. 3C). Baseline $[Ca^{2+}]_c$ was 152 ± 10 nM (n =

Table 1. Electrophysiologic Parameters in Aβ-type and C-type Dorsal Root Ganglion Neurons

	n	RMP (mV)	CV (m/s)	APamp (mV)	APd (ms)	AHPa (mV ms)
Aβ-type						
C	31	−69.6 ± 1.5	26.4 ± 1.7	73 ± 2	0.78 ± 0.05	83.0 ± 14.7
SNL	18	−67.5 ± 1.6	23.2 ± 1.2	71 ± 2	0.99 ± 0.07*	54.8 ± 13.2
C-type						
C	31	−67.3 ± 2.1	0.94 ± 0.05	87 ± 2	3.09 ± 0.26	357.4 ± 53.7
SNL	22	−62.7 ± 1.9*	0.78 ± 0.06*	77 ± 3*	3.62 ± 0.31	189.5 ± 27.6*

AHPa = afterhyperpolarization area; APamp = action potential amplitude; APd = action potential duration at 5% of peak amplitude; C = control animals; CV = conduction velocity; RMP = resting membrane potential; SNL = spinal nerve ligation animals.
* $P < 0.05$ *vs.* control (*t* test).

57), with no differences between neuronal categories. Transients recorded after retraction of the recording electrode did not differ from immediately preceding recordings during impalement ($P = 0.68$ and 0.98, n = 12), confirming that the Ca^{2+} signal is not altered by the presence of the recording electrode. Potential buffering of $[Ca^{2+}]_c$ by Fura-2 produced no effects on electrophysiologic parameters (table 1) compared with our previous findings.[24]

Single AP Axonal Stimulation Examined by Simultaneous Recording

Axonal stimulation and somatic recording of membrane potential allowed reliable generation of a single AP, accompanied by a Ca^{2+} transient with a fast upstroke and rapid monoexponential recovery (fig. 4A). Four repeated single AP stimulations produced consistent transients in C-type neurons (average difference from the mean for amplitude 6.6 ± 0.6%, n = 39; for decay time constant 7.5 ± 1.0%, n = 29; fig. 4B) and for Aδ-type neurons (amplitude 5.8 ± 1.1%, decay time constant 10.4 ± 0.8%, n = 4). The size of transients generated in response to single APs tended to be much larger for C-type neurons than faster conducting neurons (figs. 4C and D) and could not be discerned in approximately 50% of Aβ-type neurons.

Trains of APs Examined by Simultaneous Recording

Activity of sensory neuron units naturally occurs in trains of many APs,[25] which are feasible to replicate by our technique. Using only data from trains in which an AP accompanied each stimulation (for this and all following data), stability of repeated transients generated by AP trains was tested by comparing four identical trains, which demonstrated stability in Aβ-type neurons (average difference from the mean for amplitude 5.5 ± 0.9%, n = 27; decay time constant 4.5 ± 1.2%, n = 7) and in C-type neurons (amplitude 5.2 ± 1.8%, n = 5; decay time constant 4.0 ± 1.7%, n = 5), regardless of frequency and number of APs (figs. 5A and B).

Transients produced by AP trains were composed of summated responses to individual APs that could be discerned at slow firing frequencies (fig. 5C). When the unitary transient triggered by a single AP occurs before the resolution of a prior one, the cumulative stacking of $[Ca^{2+}]_c$ increments produces a higher amplitude $[Ca^{2+}]_c$ signal. This phenomenon occurred at lower stimulation frequencies in C-type neurons (usually starting at 0.3–1 Hz) than in fast conduction neurons (starting at 3–7 Hz). Further increases in frequency lessen the time available for each increment to dissipate before the next, so total transient amplitude for a burst of the same number of APs progressively increases (figs. 6A and B). We noted that an apparent maximum amplitude is reached at 50 Hz for Aβ neurons (fig. 6B). We hypothesized that once the interspike interval is shortened to the time it takes for the unitary single-AP transient to reach its peak, further increase in frequency would not produce greater stacking. Therefore, we characterized the performance of individual neurons at different frequencies. Transient amplitude continued increasing with greater AP frequency stimuli until AP conduction failed in six of the 11 C-type neurons. In the other C-type neurons and in A-type neurons (fig. 6C), a frequency was reached above which the transient amplitude did not further increase, giving each neuron a particular optimal frequency that differed on average by neuron type (medians 50 Hz for Aβ, 20 Hz for Aδ, 7 Hz for C-type, Kruskal–Wallis $P < 0.01$). Individual dissociated neurons stimulated by the impaling electrode (fig. 2B), which could not be characterized by CV, similarly showed transient amplitude maxima (20 or 50 Hz), which indicates that this tuning effect is inherent in the neuronal soma rather than deriving from a particular aspect of excitation by conducted APs or from the influences of the adjacent satellite glial cells.

Recovery of the transient after trains of 21 AP transients showed a monoexponential pattern in most neurons (C-type: 18/22, 82%; Aβ-type: 9/10, 90%) for which the decay time constant was independent of stimulation frequency ($P = 0.14$ for C-type neurons; $P = 0.13$ for Aβ-type neurons). On average, the size of transients generated in response to AP trains was larger in C-type neurons (fig. 6A) than for rapidly conducting neurons (fig. 6B).

Increasing the number of APs invading the soma should increase the total Ca^{2+} load. Therefore, we subjected neurons to trains of increasing numbers of APs at fixed stimulation frequencies. C-type neurons generally could not generate more than 30 APs at stimulation frequencies that produced stacking of unitary transients, so no data are provided. For Aβ-type neurons, increasing the number of APs from 21–400 stimuli (50 Hz) showed a logarithmic increase

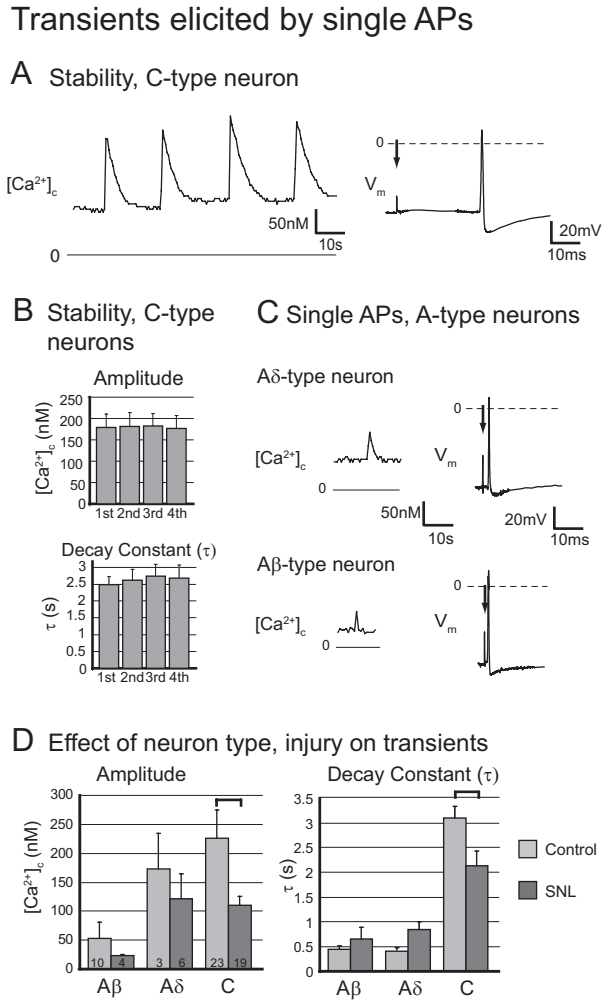

Fig. 4. Ca^{2+} transients elicited by single action potentials (APs) at 3-s intervals, recorded in neurons of intact ganglia. (*A*) Typical recording of cytosolic Ca^{2+} transients (*left*) in a control C-type neuron elicited by conducted single APs. Each of the four APs produces a comparable Ca^{2+} transient. Simultaneous recording of the membrane potential (*right*) confirms the generation of a single AP. The *arrow* indicates the artifact from dorsal root simulation. (*B*) Summary data of cytosolic Ca^{2+} transients produced by four sequential single APs in C-type neurons show no significant variation (amplitude: analysis of variance main effect $P = 0.73$, n = 39; decay constant: $P = 0.17$; n = 29). (*C*) Typical cytosolic Ca^{2+} transients and corresponding simultaneously recorded APs from an Aδ-type neuron (*upper traces*) and an Aβ-type neuron (*lower traces*) show smaller Ca^{2+} transients. (*D*) Summary data of Ca^{2+} transients elicited by a single AP in different neuron types, and comparing control neurons and neurons injured by spinal nerve ligation. The effect of injury was compared in neurons of each type separately (*t* test). *Numbers in bars* indicate n; *brackets connecting bars* indicate significant difference.

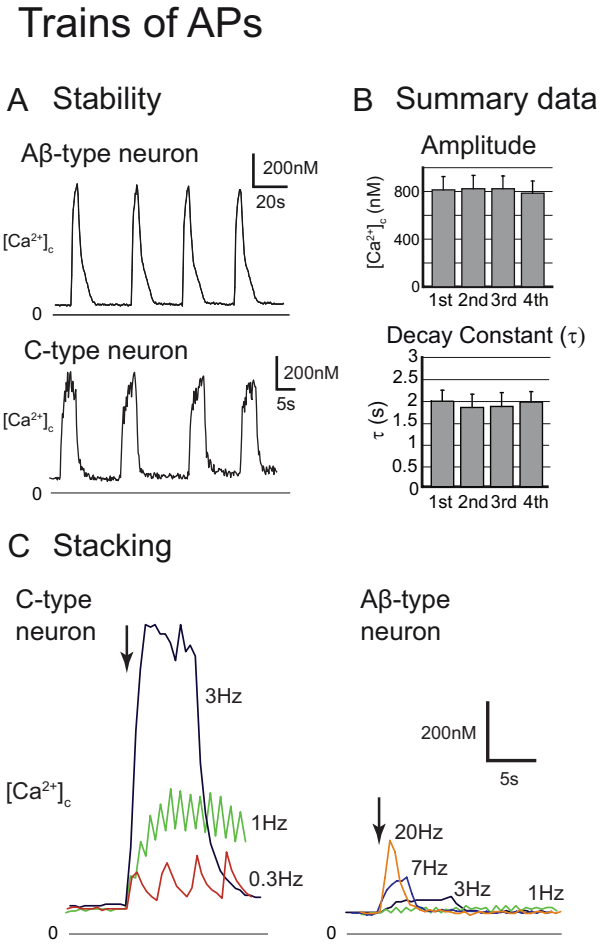

Fig. 5. Ca^{2+} transients elicited by trains of action potentials (APs) recorded in neurons of intact ganglia. (*A*) Typical recordings of cytosolic Ca^{2+} transients produced by trains of conducted APs in a control Aβ-type neuron (*upper trace*, 200 APs, 100 Hz) and in a control C-type neuron (*lower trace*, 21APs, 1 Hz). Each of the four trains produces a comparable Ca^{2+} transient. (*B*) Summary data of cytosolic Ca^{2+} transients elicited by four similar trains of APs (pooled data for frequencies that range from 7 to 100 Hz, and number of APs that range from 21 to 400) show no significant variations (Aβ-type neurons, analysis of variance main effect $P = 0.13$ for amplitude, n = 27; $P = 0.71$ for decay constant, n = 7). (*C*) Superimposed Ca^{2+} transients generated by 21 APs at different stimulation frequencies, synchronized at the onset of stimulation (*arrow*), in a C-type neuron (*left*), and an Aβ-type neuron (*right*; scale bars apply to both). The unitary Ca^{2+} events caused by individual APs stack on each other to form transients of progressively higher cumulative amplitude as stimulation frequency increases. Although accumulation of cytoplasmic Ca^{2+} is evident in the C-type neuron when stimulated as slowly as 0.3 Hz, minimal accumulation develops in the Aβ-type neuron at 1 Hz because of the small amplitude and rapid decay of the unitary transient. Only the initial portions of the stimulation period are shown for the slower stimulation frequencies.

in transient amplitude with AP number (data not shown; n = 8). This finding, together with the development of a sustained plateau during the resolving phase of the transient in all eight neurons subjected to 200 or 400 APs, suggests Ca^{2+} sequestration into intracellular compartments at higher $[Ca^{2+}]_c$.[26]

Effect of Nerve Injury Pain Model

Electrophysiologic changes induced by axotomy (table 1) duplicate the findings of our prior detailed investigation, including depolarization of the resting membrane potential,

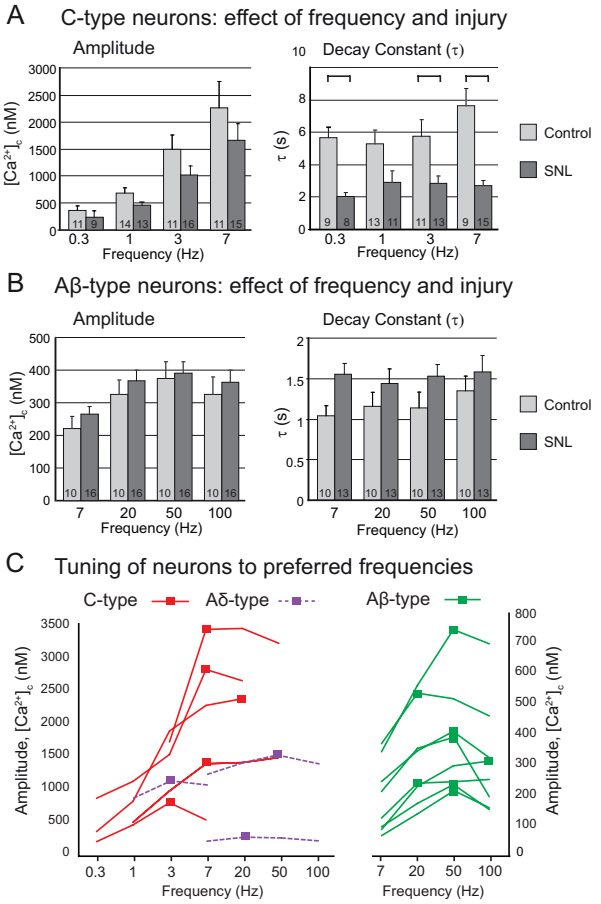

Fig. 6. The effect of stimulation frequency and prior nerve injury on cytoplasmic Ca^{2+} signals recorded in neurons of intact ganglia. (*A*) Summary data of Ca^{2+} transients produced by trains of 21 action potentials (APs) at different stimulation frequencies in C-type control neurons and in neurons injured by spinal nerve ligation. Transient amplitude increases with increasing stimulation frequency ($P < 0.001$), whereas the transient decay time constant does not change. Injured neurons display diminished transient amplitude ($P < 0.05$) and decay time constant ($P < 0.001$, analysis of variance main effects). *Numbers in bars* indicate n, *brackets connecting bars* indicate significance in paired comparison tests. (*B*) Summary data of Ca^{2+} transients produced by trains of 21 APs at different stimulation frequencies in Aβ-type control neurons and in injured neurons after spinal nerve ligation. Transient amplitude increases with stimulation frequency and reaches a maximum at 50 Hz ($P < 0.05$), whereas transient decay time constant does not change. Injury does not affect amplitude or time constant in Aβ-type neurons. *Numbers in bars* indicate n. (*C*) Individual neurons demonstrate tuning to preferred stimulation frequencies at which they produce a maximum transient amplitude. Each *line* represents a single neuron stimulated at different frequencies in a random order. The *square marker* indicates the point for each neuron at which a transient amplitude maximum is reached.

prolonged duration of APs, and diminished after hyperpolarization. Also, as previously observed, fluorometric recordings showed decreased resting $[Ca^{2+}]_c$ levels in axotomized neurons (127 ± 9 nM *vs.* 152 ± 10 nM, $P = 0.03$).

Injured C-type neurons showed substantial decrement in amplitude of transients evoked by single APs (fig. 4D) as well as by AP trains at different frequencies (fig. 6A), corroborating findings from small dissociated neurons.[9] Axotomized C-type neurons also displayed faster time constants for decay of transients evoked by single APs (fig. 4D) and in trains of APs (fig. 6A). Aδ-type neurons proved to be a heterogeneous group with highly variable transients that did not differ between control and injury groups, either with single AP stimulation (fig. 4D) or trains (data not shown). Similarly, Aβ-type neurons showed no significant differences in transients evoked by single APs (amplitude $P = 0.31$, decay constant $P = 0.5$; fig. 4D) or trains of APs (amplitude $P = 0.49$, decay constant $P = 0.12$; fig. 6B).

Discussion

The validity of cellular research depends on using appropriate experimental conditions and probes. Various means of initiating activity in neurons are used, such as K^+ application and agonist receptor binding, but exposure of cultured neurons to electrical fields has valuable attributes, including ease of use, simultaneous exposure of multiple neurons, and avoiding breech of the plasmalemma, which provides relative stability of the preparation. Dissociation of the neurons also assures that agents applied in the bath reach the neuronal membrane at a precisely known concentration. However, our findings demonstrate important disadvantages to field stimulation as a means of neuronal activation, including altered pH in the bath and uncertainty about generation of neuronal activation. In addition, stimulation is unreliable, particularly at higher rates at which neurons are able to initiate APs during direct stimulation. In response, we have adapted a technique that allows recording of cytoplasmic Ca^{2+} signals in intact neuronal tissue to the specific context of sensory neurons, providing useful particular features. Specifically, the addition of simultaneous electrophysiologic recording during the measurement of Ca^{2+} signals allows precise regulation of activity rates and patterns as well as confirmation of successful stimulation, so that comparisons between experimental conditions may be standardized. Further, neuronal health is readily verified so that data are not obtained from depolarized or nonresponsive neurons. We also incorporate the use of intact tissue, which preserves the natural functional unit of neuronal somata with their surrounding satellite glial cells.[6] Intact tissue in addition allows natural excitation of sensory neurons by AP transmission *via* the axons, thereby permitting the presentation of normal patterns of pulses. The full range of stimulation frequencies may be modeled to include natural maximal instantaneous firing frequencies for Aβ (up to 300 Hz), Aδ (up to 200 Hz), and C-type sensory neurons (up to 120 Hz).[18,27–29]

It is important to note that field stimulation has been used successfully for the study of neurons dissociated from fetal or neonatal tissue and thereafter cultured for several weeks, which results in growth of neurites.[30–32] Both these features may make the neurons more readily responsive to field stimulation, especially when the field is directly applied to the neurites.[30,31] However, adult tissue is often needed for examination of disease models, such as effects of injury, and prolonged culture may result in loss of pathologic phenotypes. Acutely dissociated DRG neurons, which lack neurites, require voltages that range from 20 to 110 V[4,9,26,33] to generate activity.

We must also specify limitations to the simultaneous recording approach. Only one neuron may be studied at a time, reducing experimental throughput. Neuronal impalement is invasive and damages the plasmalemma, although most neurons are stable for at least 30 min. Dialysis of electrolytes from the electrode may produce membrane potential shifts. To limit this effect, we used high-resistance electrodes, self-filling glass tubing stock, a modern Brown–Flaming puller, and an electrode holder with a pressure relief channel, each of which limits entry of electrolytes into the neuron.[34–36] The use of acetate as the anion rather than Cl^- minimized depolarization because of dialysis.[37] Another concern with the intracellular electrode technique is potential dialysis of small cellular metabolites, although our observation of stable membrane potential and sustained cell viability suggests an acceptable degree of this effect. The ability of bath-applied agents to penetrate into the DRG may be delayed relative to the action on a dissociated neuron, and concentrations of agents at the neuronal membrane cannot be known exactly. Finally, functional properties of the neuronal soma may only imperfectly reflect properties of membrane in other segments of the neuron.

A number of novel findings have emerged from our initial investigations with this improved recording method. The resting Ca^{2+} level of 153 ± 11 nM is higher than the levels (70–136 nM) that we and others have previously observed in dissociated neurons.[8,38–40] This higher level may result from the more natural conditions of the neurons, including lack of dissociation and examination at body temperature rather than room temperature. The Ca^{2+} transient evoked by a single AP has previously been recorded in sensory neurons,[20,41] but these previous demonstrations used dissociated neurons. Our measurement of $[Ca^{2+}]_c$ in nondissociated DRG neurons allows categorization of neurons by CV. These new observations show much larger increases in $[Ca^{2+}]_c$ elicited by single conducted APs in intact DRGs and a markedly greater Ca^{2+} signal in the probably nociceptive C-type neurons compared with the rapidly conducting A-type neurons. This difference may be attributed to the relatively prolonged AP duration of C-type neurons, which accentuates Ca^{2+} influx.[42] The $[Ca^{2+}]_c$ levels achieved by single AP activation of C-type neurons reach the range that modulate important Ca^{2+}-regulated processes, such as mitochondrial Ca^{2+} uptake, kinase activation, and short-term enhancement of synaptic transmission.[30,38,43]

We found that short trains (21 APs) generally produced Ca^{2+} transients with a high amplitude and a monoexponential recovery, whereas a discrete plateau occurred only after 100 or more APs. These findings contrast with observations from K^+-induced transients in which prolonged plateaus indicative of mitochondrial Ca^{2+} release are expected.[9] Under more physiologic Ca^{2+} loading conditions, such as we observed during natural AP excitation, shaping of the Ca^{2+} signal by intracellular Ca^{2+} sequestration into mitochondria and endoplasmic reticulum would be limited to slowly adapting sensory units exposed to sustained stimuli.

Our recordings show that AP-induced Ca^{2+} transients are larger in C-type neurons than in Aβ-type neurons, which parallels our previous finding of greater Ca^{2+} transients in large, capsaicin-insensitive neurons than in small, capsaicin-sensitive neurons. This may be due to geometrical considerations because slow-conducting neurons with small somata have a greater surface-to-volume ratio than rapidly conducting large neurons. This will result in greater accumulation of Ca^{2+} per volume of cytoplasm if current density through the plasmalemma is similar in the somata of different size, as we and others have found[10,44,45] (although others have noted greater current density in large neurons[46]). In addition, the longer AP duration of C-type neurons produces a greater duration of voltage-gated Ca^{2+} influx during each AP. The disproportionate Ca^{2+} signal in small neurons may lead to relatively greater functional plasticity despite their typically slower pulse rates.

Although Ca^{2+} transients from trains of APs in C-type neurons accumulate to higher levels than transients produced by single AP stimulation even at frequencies as low as 1 Hz (fig. 2C), this form of dynamic stacking did not occur in Aβ neurons until frequencies reached higher than 7 Hz. Furthermore, maximum transient amplitudes were achieved during trains of stimuli at much lower levels for C-type neurons than for Aβ neurons. From these new observations, it is apparent that each neuron has a dynamic response of the cytoplasmic Ca^{2+} signal that is tuned to a distinct AP frequency. Furthermore, this tuning is matched to the typical pace of neuronal activity under natural conditions, specifically transmission of high-frequency activity in rapidly conducting A-fibers and trains of low-frequency activity in slow-conducting C-type neurons.[18]

Finally, we observed distinct effects of a nerve injury pain model on Ca^{2+} signaling. In addition to decreased resting $[Ca^{2+}]_c$ levels in axotomized neurons, transient amplitude is diminished and the transient decay is accelerated after injury, but only in the presumed nociceptive C-type neurons. Accelerated Ca^{2+} clearance from injured neurons is also evident in the unitary transients that follow a single AP, which may in part explain the smaller cumulative transient amplitudes during repetitive stimulation, through diminished stacking of shorter duration unitary transients. However, our data also show that injury results in smaller transients after single

APs, indicating a contribution of decreased Ca^{2+} entry or release from stores. These observations indicate substantial disruption of processes regulating Ca^{2+} after injury, possibly accounting for hyperalgesia through increased firing of sensory neurons[24] because of diminished Ca^{2+} activation of K^+ currents.[47,48] A high degree of reliability is imparted to these findings by the use of our recording system by which we can drive neuronal activity in exact patterns and confirm the induced electrophysiologic activity, while preserving the natural structure of the DRG and avoiding injury-like artifacts of dissociation.[7] This recording approach may be particularly valuable for examination of experimental questions directly relevant to Ca^{2+} transients in the DRG somata, such as the regulation of gene expression by the temporal dynamics of the Ca^{2+} transients[31] and the increased depolarization-induced activity in DRG somata after injury.[24,49] This technique may also offer expanded research options for examining normal and diseased sensory neuron function related to clinical anesthesia, for instance, in studies considering local anesthetic toxicity, mechanisms of corticosteroid therapy for radiculopathy, and further exploration of nerve injury and other chronic pain models.

References

1. Ghosh A, Greenberg ME: Calcium signaling in neurons: Molecular mechanisms and cellular consequences. Science 1995; 268:239–47
2. Gold MS, Reichling DB, Hampl KF, Drasner K, Levine JD: Lidocaine toxicity in primary afferent neurons from the rat. J Pharmacol Exp Ther 1998; 285:413–21
3. Snutch TP, Sutton KG, Zamponi GW: Voltage-dependent calcium channels—beyond dihydropyridine antagonists. Curr Opin Pharmacol 2001; 1:11–6
4. Duflo F, Zhang Y, Eisenach JC: Electrical field stimulation to study inhibitory mechanisms in individual sensory neurons in culture. ANESTHESIOLOGY 2004; 100:740–3
5. Devor M: Unexplained peculiarities of the dorsal root ganglion. Pain 1999; (suppl 6):S27–35
6. Hanani M: Satellite glial cells in sensory ganglia: From form to function. Brain Res Brain Res Rev 2005; 48:457–76
7. Zheng JH, Walters ET, Song XJ: Dissociation of dorsal root ganglion neurons induces hyperexcitability that is maintained by increased responsiveness to cAMP and cGMP. J Neurophysiol 2007; 97:15–25
8. Fuchs A, Lirk P, Stucky C, Abram SE, Hogan QH: Painful nerve injury decreases resting cytosolic calcium concentrations in sensory neurons of rats. ANESTHESIOLOGY 2005; 102:1217–25
9. Fuchs A, Rigaud M, Hogan QH: Painful nerve injury shortens the intracellular Ca^{2+} signal in axotomized sensory neurons of rats. ANESTHESIOLOGY 2007; 107:106–16
10. Hogan QH, McCallum JB, Sarantopoulos C, Aason M, Mynlieff M, Kwok WM, Bosnjak ZJ: Painful neuropathy decreases membrane calcium current in mammalian primary afferent neurons. Pain 2000; 86:43–53
11. McCallum JB, Kwok WM, Sapunar D, Fuchs A, Hogan QH: Painful peripheral nerve injury decreases calcium current in axotomized sensory neurons. ANESTHESIOLOGY 2006; 105: 160–8
12. Kim SH, Chung JM: An experimental model for peripheral neuropathy produced by segmental spinal nerve ligation in the rat. Pain 1992; 50:355–63
13. Hogan Q, Sapunar D, Modric-Jednacak K, McCallum JB: Detection of neuropathic pain in a rat model of peripheral nerve injury. ANESTHESIOLOGY 2004; 101:476–87
14. Miller LD, Petrozzino JJ, Golarai G, Connor JA: Ca^{2+} release from intracellular stores induced by afferent stimulation of CA3 pyramidal neurons in hippocampal slices. J Neurophysiol 1996; 76:554–62
15. Sancesario G, Pisani A, D'Angelo V, Calabresi P, Bernardi G: Morphological and functional study of dwarf neurons in the rat striatum. Eur J Neurosci 1998; 10:3575–83
16. Grynkiewicz G, Poenie M, Tsien RY: A new generation of Ca^{2+} indicators with greatly improved fluorescence properties. J Biol Chem 1985; 260:3440–50
17. Villiere V, McLachlan EM: Electrophysiological properties of neurons in intact rat dorsal root ganglia classified by conduction velocity and action potential duration. J Neurophysiol 1996; 76:1924–41
18. Leem JW, Willis WD, Chung JM: Cutaneous sensory receptors in the rat foot. J Neurophysiol 1993; 69:1684–99
19. Djouhri L, Bleazard L, Lawson SN: Association of somatic action potential shape with sensory receptive properties in guinea-pig dorsal root ganglion neurones. J Physiol 1998; 513:857–72
20. Benham CD, Evans ML, McBain CJ: Ca^{2+} efflux mechanisms following depolarization evoked calcium transients in cultured rat sensory neurones. J Physiol 1992; 455: 567–83
21. Weick M, Cherkas PS, Hartig W, Pannicke T, Uckermann O, Bringmann A, Tal M, Reichenbach A, Hanani M: P2 receptors in satellite glial cells in trigeminal ganglia of mice. Neuroscience 2003; 120:969–77
22. Waddell PJ, Lawson SN, McCarthy PW: Conduction velocity changes along the processes of rat primary sensory neurons. Neuroscience 1989; 30:577–84
23. Stoney SD Jr: Unequal branch point filtering action in different types of dorsal root ganglion neurons of frogs. Neurosci Lett 1985; 59:15–20
24. Sapunar D, Ljubkovic M, Lirk P, McCallum JB, Hogan QH: Distinct membrane effects of spinal nerve ligation on injured and adjacent dorsal root ganglion neurons in rats. ANESTHESIOLOGY 2005; 103:360–76
25. Koltzenburg M, Stucky CL, Lewin GR: Receptive properties of mouse sensory neurons innervating hairy skin. J Neurophysiol 1997; 78:1841–50
26. Werth JL, Thayer SA: Mitochondria buffer physiological calcium loads in cultured rat dorsal root ganglion neurons. J Neurosci 1994; 14:348–56
27. Andrew D, Greenspan JD: Peripheral coding of tonic mechanical cutaneous pain: Comparison of nociceptor activity in rat and human psychophysics. J Neurophysiol 1999; 82:2641–8
28. Bessou P, Perl ER: Response of cutaneous sensory units with unmyelinated fibers to noxious stimuli. J Neurophysiol 1969; 32:1025–43
29. Perl ER: Myelinated afferent fibres innervating the primate skin and their response to noxious stimuli. J Physiol 1968; 197:593–615
30. Eshete F, Fields RD: Spike frequency decoding and autonomous activation of Ca^{2+}-calmodulin-dependent protein kinase II in dorsal root ganglion neurons. J Neurosci 2001; 21:6694–705
31. Fields RD, Eshete F, Stevens B, Itoh K: Action potential-dependent regulation of gene expression: Temporal specificity in Ca^{2+}, cAMP-responsive element binding proteins, and mitogen-activated protein kinase signaling. J Neurosci 1997; 17:7252–66
32. Jacobs JM, Meyer T: Control of action potential-induced Ca^{2+} signaling in the soma of hippocampal neurons by Ca^{2+} release from intracellular stores. J Neurosci 1997; 17:4129–35
33. Holz GGt, Dunlap K, Kream RM: Characterization of the

electrically evoked release of substance P from dorsal root ganglion neurons: Methods and dihydropyridine sensitivity. J Neurosci 1988; 8:463–71

34. Stoner LC, Natke E Jr, Dixon MK: Direct measurement of potassium leak from single 3 M KCl microelectrodes. Am J Physiol 1984; 246:F343–8
35. Isenberg G: Risk and advantages of using strongly beveled microelectrodes for electrophysiological studies in cardiac Purkinje fibers. Pflügers Arch 1979; 380:91–8
36. Fromm M, Schultz SG: Some properties of KCl-filled microelectrodes: Correlation of potassium "leakage" with tip resistance. J Membr Biol 1981; 62:239–44
37. Blatt MR, Slayman CL: KCl leakage from microelectrodes and its impact on the membrane parameters of a nonexcitable cell. J Membr Biol 1983; 72:223–34
38. Thayer SA, Miller RJ: Regulation of the intracellular free calcium concentration in single rat dorsal root ganglion neurones *in vitro.* J Physiol 1990; 425:85–115
39. Stucky CL, Abrahams LG, Seybold VS: Bradykinin increases the proportion of neonatal rat dorsal root ganglion neurons that respond to capsaicin and protons. Neuroscience 1998; 84:1257–65
40. Huang TJ, Sayers NM, Fernyhough P, Verkhratsky A: Diabetes-induced alterations in calcium homeostasis in sensory neurones of streptozotocin-diabetic rats are restricted to lumbar ganglia and are prevented by neurotrophin-3. Diabetologia 2002; 45:560–70
41. Cohen AS, Moore KA, Bangalore R, Jafri MS, Weinreich D, Kao JP: Ca(2+)-induced Ca^{2+} release mediates Ca^{2+} transients evoked by single action potentials in rabbit vagal afferent neurones. J Physiol 1997; 499:315–28
42. Toth PT, Miller RJ: Calcium and sodium currents evoked by action potential waveforms in rat sympathetic neurones. J Physiol 1995; 485:43–57
43. Regehr WG, Delaney KR, Tank DW: The role of presynaptic calcium in short-term enhancement at the hippocampal mossy fiber synapse. J Neurosci 1994; 14:523–37
44. Abdulla FA, Smith PA: Axotomy- and autotomy-induced changes in the excitability of rat dorsal root ganglion neurons. J Neurophysiol 2001; 85:630–43
45. Abdulla FA, Smith PA: Axotomy- and autotomy-induced changes in Ca^{2+} and K^{+} channel currents of rat dorsal root ganglion neurons. J Neurophysiol 2001; 85:644–58
46. Lu SG, Zhang X, Gold MS: Intracellular calcium regulation among subpopulations of rat dorsal root ganglion neurons. J Physiol 2006; 577:169–90
47. Hogan Q, Lirk P, Poroli M, Rigaud M, Fuchs A, Fillip P, Ljubkovic M, Gemes G, Sapunar D: Restoration of calcium influx corrects membrane hyperexcitability in injured rat dorsal root ganglion neurons. Anesth Analg 2008; 107:1045–51
48. Lirk P, Poroli M, Rigaud M, Fuchs A, Fillip P, Huang CY, Ljubkovic M, Sapunar D, Hogan Q: Modulators of calcium influx regulate membrane excitability in rat dorsal root ganglion neurons. Anesth Analg 2008; 107:673–85
49. Zhang JM, Song XJ, LaMotte RH: Enhanced excitability of sensory neurons in rats with cutaneous hyperalgesia produced by chronic compression of the dorsal root ganglion. J Neurophysiol 1999; 82:3359–66